CONCRETE LIBRARY OF JSCE NO. 29, JUNE 1997

MATHEMATICAL MODELING FOR PERMEABILITY BEHAVIOR OF NON-HOMOGENEOUS MATERIAL AND ITS APPLICABILITY

(Translation from Proceeding of JSCE, No.526 / V-29, November 1995)

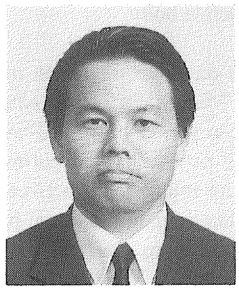

Hideki OSHITA

Tada-aki TANABE

A mathematical model for water migration in concrete of which properties are changes from homogeneous to non homogeneous material applied the loading history, is presented in detail. Then, its applicability is confirmed by comparing predictions with experimental results and the relationship between crack width and coefficient of permeability is investigated. In the proposed model, concrete comprising aggregate, cement paste, water, interfacial cracks between aggregate and cement paste, and a crack band is assumed to be a composite material, and discontinuities in displacement and hydraulic gradient at cracks are taken into account in detail.

Keywords: *water migration, coefficient of permeability, homogeneous material, non homogeneous material, pore water pressure, effective stress, total stress, crack width, leakage water*

Hideki Oshita is an Assistant Professor in the Department of Civil Engineering at the National Defense Academy, Yokosuka, Japan. He obtained his Dr. Eng. from Nagoya University in 1995. His research interests relate to the characteristics of water migration in concrete and the deformation mechanism of composite structures. He is a member of the JSCE and JCI.

Tada-aki Tanabe is a Professor in the Department of Civil Engineering at Nagoya University, Nagoya, Japan. He obtained his Dr. Eng. from Tokyo University in 1971. His research interests include thermal stress behavior, characteristics of water migration, and constitutive equations for young and hardened concrete. He is a member of the JSCE, JCI, RILEM, and IYBSE.

1. INTRODUCTION

A recent focus of civil engineering is to utilize concrete structures such as deep underground structures and marine structures. However, the water tightness of concrete, especially the problem of leakage through cracks, greatly influences not only structural stability and aesthetics, but also corrosion. For example, in the design of a facility radioactive waste for the disposal of produced in a nuclear power plant, it is important to check for leakage problems. Such problems result from water migration in concrete as a homogeneous and non-homogeneous material. Water migration in concrete occurs dominantly through cracks such as micro and macro cracks rather than uniformly through voids, and so to estimate the characteristics of water migration it is essential to treat concrete as a non-homogeneous concrete body.

Representative studies on water migration in concrete as a homogeneous material were performed by J.Murata[1] and T.C.Powers[2]. J.Murata performed extensive permeability experiments on hardened concrete and reported a the relationship between permeability and water-cement ratio with the maximum size of aggregate as a parameter. T.C.Powers performed permeability experiments a early-age and hardened concrete with a water-cement ratio of 0.70 and reported a the relationship between permeability and age. Both these studies on permeability are very useful as a means of determining the initial permeability of concrete as a homogeneous material. On the other hand, studies on water migration in concrete as a non-homogeneous material have been performed by Ishikawa[3], Watabe[4], and Ito et al.[5]. They performed leakage experiments a concrete with a single crack and reported similar experimental formulas for leakage as a function of specimen size, coefficient of viscosity, crack parameter, and external pressure. Ishikawa and Watabe demonstrated the applicability of their proposed formula through experiments at low external pressure (below 2kPa) while Ito showed applicability at high external pressure (above 20kPa). However, a crack parameter defined as a material constant expressing watercourse length, frictional resistance, and tortuosity due to crack roughness is needed in each proposed formula, and the value of this constant raries widely even with the same concrete mix, that is, the crack parameter is an uncertain factor. Consequently, it can be said that, there is no unified formula for water migration in concrete as a non-homogeneous material. Further, the cracks occurring in concrete structures under the action of external loading are of smeared type, meaning there are many passing and surface cracks. Therefore, the total water leakage can not be defined as the sum of the results obtained by using these formulas on each crack. It therefore appears that to estimate of water leakage analytically, the relationship between crack pattern and permeability is most important, rather than the relationship between crack width and water leakage. Hence permeability at the macro level for a concrete body having homogeneous and non-homogeneous areas must be investigated.

In this study, a mathematical model of water migration in concrete with both homogeneous and non-homogeneous characteristics resulting from external loading, was developed and the applicability of the model to local water migration, i.e. water migration in cracks, is examined. In the practical calculation, at first, the material parameters in the developed model and the permeability in concrete as a non homogeneous material was decided due to the application of the developed model to the experimental results performed by Watabe. Then, using the permeability obtained by analysis, the applicability of the developed model is examined thorough comparison with the experimental results obtain by Ito et al. and finally relationship between permeability and crack width for concrete as a non-homogeneous material was proposed.

2. MODELING OF CONCRETE AS A NON-HOMOGENEOUS MATERIAL

Concrete as a non-homogeneous material is assumed to be a porous composite material is consisting of aggregate, cement paste, water, and interfacial cracks occurring at interfaces between aggregate and cement paste and at interfaces between cement paste and the crack band forming the fracture surface, as shown in Fig.1. The concrete model is shown in Fig.2 and cracks occurring in the concrete body are a two-crack pattern of the crack band and interfacial cracks. In the model the aggregate, cement paste, water, interfacial cracks, and crack band are denoted by A, C, W, IC, CB, respectively. The symbols $V^{(A)}, V^{(C)}, V^{(CB)}$ shown in Fig.2 denote the volume of aggregate, cement paste, and crack band and the symbols S, S_{A-C}, S_{C-CB} denote the surface area of the concrete body, the interfacial surface area of aggregate and cement paste, of cement paste and crack band. The permeability matrix and elasto-plastic matrix for a concrete body with cracks was developed due to the estimation of discontinuities in the hydraulic gradient and displacement at the crack surface on a micro level. Then an analytical theory for water migration in concrete as a non-homogeneous material was developed due to the coupling the mass conservation law and force equilibrium equation, as shown in Figs.2 and 3.

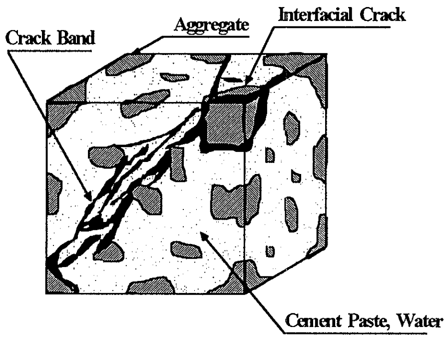

Fig. 1 Concrete as Non-homogeneous Material

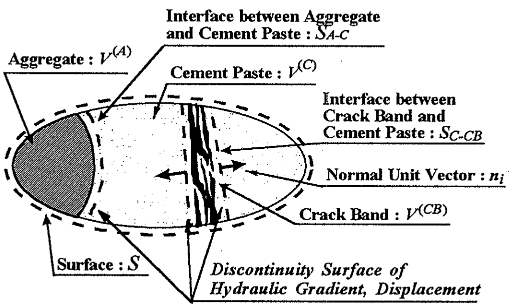

FIG. 3. Modeling of Concrete as Non-homogeneous Material

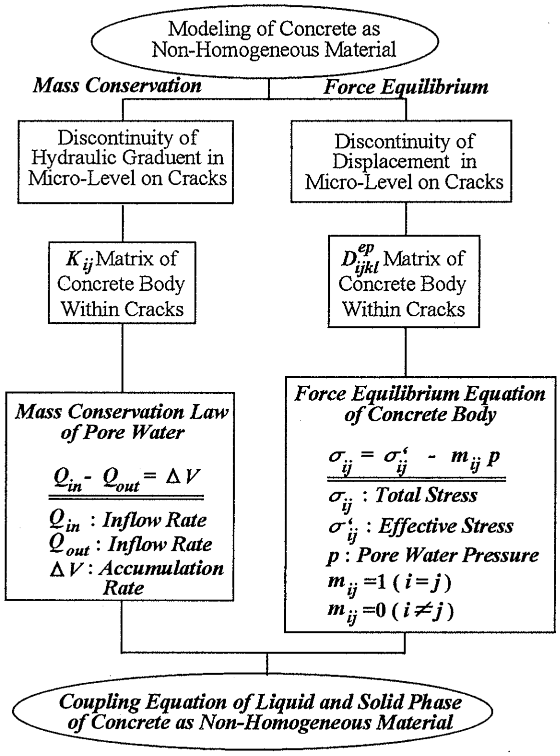

Fig. 4 Flowchart of Modeling of Concrete

2.1 Formulation of Permeability Matrix

The increment in the average hydraulic gradient vector on the macro level, $d\bar{\iota}_i$, can be written using the incremental hydraulic gradient vector on the micro level, $d\iota_i$, as

$$d\bar{\iota}_i = \frac{1}{V}\int_V d\iota_i \, dV \tag{1}$$

where the symbol V is the controlled volume. Equation.(1) can be decomposed into the components shown in Fig.2 as

$$d\bar{\iota}_i = C_1 \cdot d\bar{\iota}_i^{(A)} + C_2 \cdot d\bar{\iota}_i^{(C)} + C_3 \cdot d\bar{\iota}_i^{(CB)} + X_i \tag{2}$$

where the symbols C_1, C_2, C_3 are the ratio of aggregate, cement paste, and crack band volumes to the controlled volume and the vectors $d\bar{\iota}_i^{(A)}, d\bar{\iota}_i^{(C)}, d\bar{\iota}_i^{(CB)}$ denote the increments in average hydraulic gradient vector on the micro level in the aggregate, cement paste, and crack band as given by.

$$d\bar{\iota}_i^{(\alpha)} = \frac{1}{V^{(\alpha)}} \int_{V^{(\alpha)}} d\iota_i^{(\alpha)} \, dV \tag{3}$$

where the variable α denotes the aggregate A, cement paste C, and crack band CB.
The vector X_i denotes the discontinuity in hydraulic gradient at each interface, as shown in Fig.2, becoming zero similarly to $d\bar{\iota}_i^{(CB)}$ before cracking. The increment in average hydraulic gradient vectors $d\bar{\iota}_i^{(\alpha)}$ $(\alpha = A, C, CB)$ on the left-hand side of Eq.(3) can be written using the increment in total water head, $dh^{(\alpha)}$, as

$$d\bar{\iota}_i^{(\alpha)} = \nabla_i dh^{(\alpha)} = dh_{,i}^{(\alpha)} \tag{4}$$

$$dh^{(\alpha)} = dz^{(\alpha)} + \frac{dP^{(\alpha)}}{\gamma_W}$$

where γ_w is the weight per unit volume of water. Substituting Eqs.(3) and (4) into Eq.(2), the summation of the right-hand side X_i of Eq.(2) except for can be written as

$$\begin{aligned} & C_1 \cdot d\bar{\iota}_i^{(A)} + C_2 \cdot d\bar{\iota}_i^{(C)} + C_3 \cdot d\bar{\iota}_i^{(CB)} = \\ & \frac{1}{V}\left(\int_{V^{(A)}} dh_{,i}^{(A)} dV + \int_{V^{(C)}} dh_{,i}^{(C)} dV + \int_{V^{(CB)}} dh_{,i}^{(CB)} dV \right) \end{aligned} \tag{5}$$

Substituting Gauss's divergent theory given as the following equation

$$\int_V \nabla_i dh \, dV = \int_V dh_{,i} \, dV = \int_S dhn_i \, dS \tag{6}$$

into each term on the right hand side of Eq.(5) and assuming the direction of the outer normal vector n_i at the crack band surface to be positive as shown in Fig.2, Eq.(5) can be rewritten as

$$\begin{aligned} & C_1 \cdot d\bar{\iota}_i^{(A)} + C_2 \cdot d\bar{\iota}_i^{(C)} + C_3 \cdot d\bar{\iota}_i^{(CB)} = \\ & \qquad \frac{1}{V}\int_S dh \, n_i dS + \frac{1}{V}\int_{S^{A-C}} [dh]_A^C n_i \, dS \\ & \qquad + \frac{2}{V}\int_{S^{C-CB}} [dh]_C^{CB} n_i \, dS \end{aligned} \tag{7}$$

where $[dh]_A^C, [dh]_C^{CB}$ denote the discontinuity in total water head between the aggregate and cement paste and between the cement paste and crack band, respectively.

The first term on the right-hand side of Eq.(7) represents the increment in average hydraulic gradient vector on the macro level, $d\bar{\iota}_i$, on the basis of Eq.(6) and can be rewritten as

$$\begin{aligned} d\bar{\iota}_i = & C_1 \cdot d\bar{\iota}_i^{(A)} + C_2 \cdot d\bar{\iota}_i^{(C)} + C_3 \cdot d\bar{\iota}_i^{(CB)} \\ & - \frac{1}{V}\int_{S^{A-C}} [dh]_A^C n_i \, dS \\ & - \frac{2}{V}\int_{S^{C-CB}} [dh]_C^{CB} n_i \, dS \end{aligned} \tag{8}$$

Therefore, comparing with Eq.(2) and Eq.(8), the vector X_i in Eq.(2) can be defined as the summation of the fourth and fifth terms on the right-hand side of Eq.(8). Now, the incremental hydraulic gradient vector, $d\iota_i$, at the crack surface as shown in Fig.4 is defined as

$$d\iota_i = d\iota_n n_i + d\iota_t t_i \tag{9}$$

where $d\iota_n, d\iota_t$ are the components of hydraulic gradient in the normal and horizontal directions at the crack surface, respectively.

Secondly, the discontinuities in total water head $[dh]_A^C, [dh]_C^{CB}$ are defined as

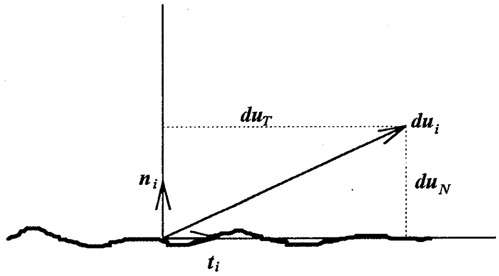

Fig. 6 Component of Displacement on Crack Surface

$$\begin{aligned} [dh]_A^C &= V \cdot a \cdot \omega \cdot d\bar{\iota}_n \\ [dh]_C^{CB} &= V/2 \cdot b \cdot \omega \cdot d\bar{\iota}_n \end{aligned} \tag{10}$$

where a,b denote the degree of discontinuity, i.e., the material parameter which expresses the degree of reducing ratio of hydraulic gradient with crack width and ω is the damage parameter[6].

The components of hydraulic gradient $d\bar{\iota}_n$ in the normal direction at the crack surface can be written using the increment in average hydraulic gradient vector on the macro level, $d\bar{\iota}_i$, as

$$d\bar{\iota}_n = d\bar{\iota}_i \cdot n_i \tag{11}$$

Substituting Eqs.(10) and (1) into Eq.(8) and assuming the ratio of crack band volume to controlled volume to be zero $(C_3 = 0)$, Eq.(8) can be written as

$$d\bar{\iota}_i = C_1 \cdot d\bar{\iota}_i^{(A)} + C_2 \cdot d\bar{\iota}_i^{(C)} - A_{ij} d\bar{\iota}_j - B_{ij} d\bar{\iota}_j \tag{12}$$

where the matrices A_{ij}, B_{ij} which denote the degree of the discontinuity of hydraulic gradient due to cracks can be written as

$$\begin{aligned} A_{ij} &= \int_{S^{A-C}} c\,\omega\,\gamma_{ij}\, dS \\ B_{ij} &= \int_{S^{C-CB}} d\,\omega\,\gamma_{ij}\, dS \\ \gamma_{ij} &= n_i n_j \end{aligned} \tag{13}$$

Moreover, applying the Micro Plane Model[7] to the surface integration in Eq.(13), many cracks can be estimated at the same time and Eq.(13) can be rewritten as

$$\begin{aligned} A_{ij} &= \int_0^{2\pi} c\,\omega\,\gamma_{ij} A_t^{A-C} \Omega^{A-C}(\theta)\, d\theta \\ B_{ij} &= \int_0^{2\pi} d\,\omega\,\gamma_{ij} A_t^{C-CB} \Omega^{C-CB}(\theta)\, d\theta \end{aligned} \tag{14}$$

where $\Omega^{A-C}(\theta), \Omega^{C-CB}(\theta)$ are the contact density function of cracks at the interface of aggregate and cement paste and at the interface of cement paste and crack band, respectively. A_t^{A-C}, A_t^{C-CB} are the whole surface area per unit crack plane, respectively. In this way, applying the Micro Plane Model to the surface integration, the discontinuity in hydraulic gradient not only at a single crack but at many cracks can be estimated.

Substituting Darcy's law as given in the following equation

$$
\begin{aligned}
d\bar{v}_i^{(A)} &= K_{ij}^{(A)} d\bar{\imath}_j^{(A)} \\
d\bar{v}_i^{(C)} &= K_{ij}^{(C)} d\bar{\imath}_j^{(C)}
\end{aligned}
\tag{15}
$$

into the increment in average hydraulic gradient vector a the micro level, $d\bar{\imath}_i^{(A)}, d\bar{\imath}_i^{(C)}$, in the first and second terms on the right-hand side of Eq.(12), Eq.(12) can be rewritten as

$$
\begin{aligned}
d\bar{\imath}_i = & C_1 \cdot K_{ik}^{(A)^{-1}} d\bar{v}_k^{(A)} + C_2 \cdot K_{ik}^{(C)^{-1}} d\bar{v}_k^{(C)} \\
& - A_{ij} d\bar{\imath}_j - B_{ij} d\bar{\imath}_j
\end{aligned}
\tag{16}
$$

where the matrices $K_{ij}^{(A)}, K_{ij}^{(C)}$ are the permeability matrix of aggregate and cement paste, respectively and the vectors $d\bar{v}_i^{(A)}, d\bar{v}_i^{(C)}$ are the increment in average flow velocity on the micro level in the aggregate and cement paste, respectively.

Transferring the subscript of hydraulic gradient vector $d\bar{\imath}_i$ in Eq.(16) i to j, Eq.(16) can be written as

$$
\begin{aligned}
\delta_{ij} d\bar{\imath}_j = & C_1 \cdot K_{ik}^{(A)^{-1}} d\bar{v}_k^{(A)} + C_2 \cdot K_{ik}^{(C)^{-1}} d\bar{v}_k^{(C)} \\
& - A_{ij} d\bar{\imath}_j - B_{ij} d\bar{\imath}_j
\end{aligned}
\tag{17}
$$

Transferring the third and fourth terms at the right-hand side of Eq.(17) to the left-hand side, Eq.(17) can be written as

$$
Q_{ij} d\bar{\imath}_j = C_1 \cdot K_{ik}^{(A)^{-1}} d\bar{v}_k^{(A)} + C_2 \cdot K_{ik}^{(C)^{-1}} d\bar{v}_k^{(C)} \tag{18}
$$

where the matrix Q_{ij} denotes the rate of reduction in hydraulic gradient due to cracks and can be written as

$$
Q_{ij} = \delta_{ij} + A_{ij} + B_{ij} \tag{19}
$$

Now, the relation between the increment in average flow velocity vector on the macro level, $d\bar{v}_i$, and the vector on the micro level, $d\bar{v}_i^{(\alpha)}$ $(\alpha = A, C)$, is defined as

$$
d\bar{v}_i^{(\alpha)} = C_{ij}^{(\alpha)} d\bar{v}_j \qquad \alpha = A, C \tag{20}
$$

where the matrix $C_{ij}^{(\alpha)}$ $(\alpha = A, C)$ is defined as the concentration matrix of flow velocity. The increment in average flow velocity vector on the macro level, $d\bar{v}_i$, can be written similarly to Eq.(1) and (2) using the incremental flow velocity on the micro level, dv_i, and the increment in average flow velocity on the micro level, $d\bar{v}_i^{(\alpha)}$, as

$$
d\bar{v}_i = \frac{1}{V} \int_V dv_i \, dV = C_1 \cdot d\bar{v}_i^{(A)} + C_2 \cdot d\bar{v}_i^{(C)} \tag{21}
$$

In Eq.(21), it should be noted that the continuous changes in flow velocity at each interface as shown in Fig.2 occur and the ratio of crack band volume to controlled volume is already equal to zero ($C_3 = 0$). Substituting Eq.(20) into Eq.(21), the relation between the concentration matrices of the aggregate and cement paste can be written as

$$C_1 C_{ij}^{(A)} + C_2 C_{ij}^{(C)} = I_{ij} \tag{22}$$

where the matrix I_{ij} is the unit matrix.

Moreover, substituting Eq.(20) into Eq.(18), Eq.(18) can be rewritten as

$$Q_{ij} d\bar{i}_j = \left(C_1 \cdot K_{ik}^{(A)^{-1}} C_{kl}^{(A)} + C_2 \cdot K_{ik}^{(C)^{-1}} C_{kl}^{(C)} \right) d\bar{v}_l \tag{23}$$

Finally, the permeability matrix of a concrete body on the macro level, which is related by the increment in average flow velocity vector on the macro level, $d\bar{v}_i$, and the increment in average hydraulic gradient vector on the macro level, $d\bar{i}_i$, can be written as

$$K_{ij} = \left(C_1 \cdot K_{il}^{(A)^{-1}} C_{lm}^{(A)} + C_2 \cdot K_{il}^{(C)^{-1}} C_{lm}^{(C)} \right)^{-1} Q_{mj} \tag{24}$$

Solving the simultaneous equations Eq.(22) and Eq.(24), the concentration matrix of flow velocity $C_{ij}^{(A)}, C_{ij}^{(C)}$ which appear in Eq.(24) can be written as

$$\begin{aligned} C_{ij}^{(C)} &= \left\{ C_2 \cdot \left(K_{ik}^{(C)^{-1}} - K_{ik}^{(A)^{-1}} \right) \right\}^{-1} \\ &\qquad \left(Q_{kl} - K_{km}^{(A)^{-1}} K_{ml} \right) K_{lj}^{-1} \\ C_{ij}^{(A)} &= \left(I_{ij} - C_2 \cdot C_{ij}^{(C)} \right) / C_1 \end{aligned} \tag{25}$$

Analysis proceeds as follows. The concentration matrices shown as Eq.(25) are updated by substituting the permeability matrix just at before step and, by substituting the updated concentration matrices into the permeability matrix shown as Eq.(24), the permeability matrix is updated. Finally, the unbalanced flow rate is calculated from the outflow rate calculated using the current permeability matrix and outflow rate as a external terms. Further, the calculation is iterated until the error in the unbalanced flow rate specific value by the modified Newton Raphson method.

2.2 Formulation of Elasto Plastic Stiffness Matrix

The increment in average strain at the macro level, $d\bar{\varepsilon}_{ij}$, can be written using the incremental strain on the micro level, $d\varepsilon_{ij}$, as

$$d\bar{\varepsilon}_{ij} = \frac{1}{V} \int_V d\varepsilon_{ij} \, dV \tag{26}$$

Equation.(16) can be written by decomposing the components shown in Fig.2 as

$$d\bar{\varepsilon}_{ij} = C_1 \cdot d\bar{\varepsilon}_{ij}^{(A)} + C_2 \cdot d\bar{\varepsilon}_{ij}^{(C)} + C_3 \cdot d\bar{\varepsilon}_{ij}^{(CB)} + X_{ij} \tag{27}$$

where $d\bar{\varepsilon}_{ij}^{(A)}, d\bar{\varepsilon}_{ij}^{(C)}, d\bar{\varepsilon}_{ij}^{(CB)}$ denote the increment in average strain on the micro level for the aggregate, cement paste, and crack band respectively, as represented by the following equation:

$$d\bar{\varepsilon}_{ij}^{(\alpha)} = \frac{1}{V^{(\alpha)}} \int_{V^{(\alpha)}} d\varepsilon_{ij}^{(\alpha)}\, dV \qquad \alpha = A, C, CB \tag{28}$$

The second order tensor X_{ij} denotes the strain discontinuity at each interface and becomes zero similarly to the increment of average strain on the micro level of the crack band $d\bar{\varepsilon}_{ij}^{(CB)}$ before cracking, as shown in Fig.2. Substituting the relation between strain and displacement into the increment of average strain on the micro level $d\bar{\varepsilon}_{ij}^{(\alpha)}$ $(\alpha = A, C, CB)$ of the first to third terms on the right-hand side of Eq.(27), the summation of the right-hand side except for X_{ij} in Eq.(27) can be written as

$$\begin{aligned} C_1 \cdot d\bar{\varepsilon}_{ij}^{(A)} + C_2 \cdot d\bar{\varepsilon}_{ij}^{(C)} + C_3 \cdot d\bar{\varepsilon}_{ij}^{(CB)} = \\ \frac{1}{V}\{\frac{1}{2}\int_{V^{(A)}} (du_{i,j}^{(A)} + du_{j,i}^{(A)})\, dV + \\ \frac{1}{2}\int_{V^{(C)}} (du_{i,j}^{(C)} + du_{j,i}^{(C)})\, dV + \\ \frac{1}{2}\int_{V^{(CB)}} (du_{i,j}^{(CB)} + du_{j,i}^{(CB)})\, dV\} \end{aligned} \tag{29}$$

where the vectors $d\bar{u}_i^{(\alpha)}$ $(\alpha = A, C, CB)$ denote the incremental displacement a the micro level of aggregate, cement paste, and the crack band, respectively.

Substituting Gauss's divergent theory into each term on the right-hand side of Eq.(29) and assuming the direction of the outer normal vector n_i at the crack band surface is positive as shown in Fig.2, Eq.(29) can be rewritten as

$$\begin{aligned} C_1 \cdot d\bar{\varepsilon}_{ij}^{(A)} + C_2 \cdot d\bar{\varepsilon}_{ij}^{(C)} + C_3 \cdot d\bar{\varepsilon}_{ij}^{(CB)} = \\ \frac{1}{V}\frac{1}{2}\int_{S} (du_i n_j + du_j n_i)\, dS + \\ \frac{1}{2V}\int_{S^{A-C}} ([du_i]_A^C n_j + [du_j]_A^C n_i)\, dS + \\ \frac{1}{V}\int_{S^{C-CB}} ([du_i]_C^{CB} n_j + [du_j]_C^{CB} n_i)\, dS \end{aligned} \tag{30}$$

where $[du_i]_A^C, [du_i]_C^{CB}$ denote the discontinuity in the incremental displacement vector between aggregate and cement paste and between cement paste and the crack band, respectively. The first term of the right-hand side of Eq.(30) represents the increment in average strain on the macro level, $d\bar{\varepsilon}_{ij}$, i.e., Eq.(26) and Eq.(30) can be rewritten as

$$d\bar{\varepsilon}_{ij} = C_1 \cdot d\bar{\varepsilon}_{ij}^{(A)} + C_2 \cdot d\bar{\varepsilon}_{ij}^{(C)} + C_3 \cdot d\bar{\varepsilon}_{ij}^{(CB)} - \frac{1}{2V}\int_{S^{A-C}} \left([du_i]_A^C n_j + [du_j]_A^C n_i \right) dS - \frac{1}{V}\int_{S^{C-CB}} \left([du_i]_C^{CB} n_j + [du_j]_C^{CB} n_i \right) dS \tag{31}$$

Therefore, comparing with Eq.(27) and (31), the second-order tensor X_{ij} in Eq.(27) can be defined as the summation of the fourth and fifth terms on the right-hand side of Eq.(31). Now, the incremental displacement vector du_i at the crack surface as shown in Fig.5 is defined as

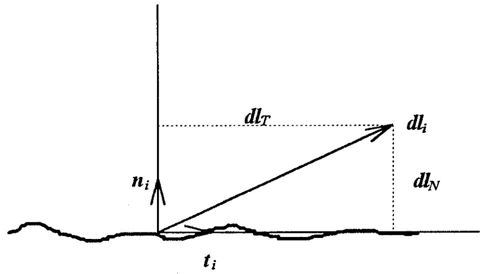

Fig. 5 Component of hydraulic Gradient on Crack Surface

$$du_i = du_n n_i + du_t t_i \tag{32}$$

where du_n, du_t are the component of displacement in the normal and horizontal directions at each crack surface, respectively. Substituting Eq.(32) into Eq.(31) and the ratio of volume of the crack band to the controlled volume is assumed to be zero ($C_3 = 0$), Eq.(31) can be written as

$$\begin{aligned} d\bar{\varepsilon}_{ij} &= C_1 \cdot d\bar{\varepsilon}_{ij}^{(A)} + C_2 \cdot d\bar{\varepsilon}_{ij}^{(C)} - \frac{1}{V}\int_{S^{A-C}} [du_n]_A^C \alpha_{ij}\, dS \\ &- \frac{1}{2V}\int_{S^{A-C}} [du_t]_A^C \beta_{ij}\, dS - \frac{2}{V}\int_{S^{C-CB}} [du_n]_C^{CB} \alpha_{ij}\, dS \\ &- \frac{1}{V}\int_{S^{C-CB}} [du_t]_C^{CB} \beta_{ij}\, dS \\ \alpha_{ij} &= n_i n_j \\ \beta_{ij} &= t_i n_j + n_i t_j \end{aligned} \tag{33}$$

where $[du_n]_A^C, [du_t]_A^C$ and $[du_n]_C^{CB}, [du_t]_C^{CB}$ denote the discontinuity in incremental displacement in the normal and horizontal directions at the crack surface between aggregate and cement paste and between cement paste and the crack band, respectively.

Now, the above discontinuities of incremental displacement $[du_n]_A^C, [du_t]_A^C, [du_n]_C^{CB}, [du_t]_C^{CB}$ are defined as

$$\begin{aligned} [du_n]_A^C &= V \cdot \omega_1 \cdot d\varepsilon_n \\ [du_t]_A^C &= 2V \cdot \omega_2 \cdot d\varepsilon_t \\ [du_n]_C^{CB} &= \frac{V}{2} \cdot \omega_1 \cdot d\varepsilon_n \\ [du_t]_C^{CB} &= V \cdot \omega_2 \cdot d\varepsilon_t \end{aligned} \tag{34}$$

where $d\varepsilon_n, d\varepsilon_t$ denote the components of strain in the normal and horizontal directions at the crack surface and ω_1, ω_2 are defined as

$$\omega_1 = e^{\left(\frac{d\varepsilon_n}{c}\right)} - 1$$
$$\omega_2 = e^{\left(\frac{d\varepsilon_t}{d}\right)} - 1 \tag{35}$$

where c,d represent the degree of discontinuity, i.e., they are material parameters which express the degree of strain localization due to cracks. Hence, ω_1, ω_2 are parameters related by the increment in average strain on the macro level and crack width on the micro level. Moreover, the components of strain in the normal and horizontal direction $d\varepsilon_n, d\varepsilon_t$ can be written using the increment in average strain on the macro level, $d\bar{\varepsilon}_{ij}$, as

$$d\varepsilon_n = d\bar{\varepsilon}_{ij} \cdot n_i \cdot n_j$$
$$d\varepsilon_t = d\bar{\varepsilon}_{ij} \cdot \left(t_i n_j + n_i t_j\right) / 2 \tag{36}$$

Substituting Eq.(34)～(36) into Eq.(33), Eq.(33) can be rewritten as

$$d\bar{\varepsilon}_{ij} = C_1 \cdot d\bar{\varepsilon}_{ij}^{(A)} + C_2 \cdot d\bar{\varepsilon}_{ij}^{(C)} - A'_{ijkl}\, d\bar{\varepsilon}_{kl} - B'_{ijkl}\, d\bar{\varepsilon}_{kl} \tag{37}$$

where the matrices A'_{ij} , B'_{ij} which denote the degree of strain discontinuity due to cracks, can be written as

$$A'_{ijkl} = \int_{S^{A-C}} (\omega_1 \alpha'_{ijkl} + \omega_2 \beta'_{ijkl})\, dS$$
$$B'_{ijkl} = \int_{S^{C-CB}} (\omega_1 \alpha'_{ijkl} + \omega_2 \beta'_{ijkl})\, dS \tag{38}$$
$$\alpha'_{ijkl} = n_i n_j n_k n_l$$
$$\beta'_{ijkl} = (t_i n_j + n_i t_j)(t_k n_l + n_k t_l) / 2$$

Here, applying the Micro Plane Model as with Eq.(14) to carry at a surface integration and estimate multiple cracks at the same time, Eq.(38) can be written as

$$A'_{ijkl} = \int_0^{2\pi} (\omega_1 \alpha'_{ijkl} + \omega_2 \beta'_{ijkl}) A_t^{A-C}\, \Omega^{A-C}(\theta)\, d\theta$$
$$B'_{ijkl} = \int_0^{2\pi} (\omega_1 \alpha'_{ijkl} + \omega_2 \beta'_{ijkl}) A_t^{C-CB}\, \Omega^{C-CB}(\theta)\, d\theta \tag{39}$$

Substituting the relation between stress and strain shown by the following equations

$$d\bar{\sigma}_{ij}^{(A)} = D_{ijkl}^{(A)}\, d\bar{\varepsilon}_{kl}^{(A)}$$
$$d\bar{\sigma}_{ij}^{(C)} = D_{ijkl}^{(C)}\, d\bar{\varepsilon}_{kl}^{(C)} \tag{40}$$

into the increments in average strain on the micro level $d\bar{\varepsilon}_{ij}^{(A)}, d\bar{\varepsilon}_{ij}^{(C)}$ of the first and second terms on the right-hand side of Eq.(37), Eq.(37) can be rewritten as

$$d\bar{\varepsilon}_{ij} = C_1 \cdot {D_{ijmn}^{(A)}}^{-1} d\bar{\sigma}_{mn}^{(A)} + C_2 \cdot {D_{ijmn}^{(C)}}^{-1} d\bar{\sigma}_{mn}^{(C)}$$
$$- A'_{ijkl}\, d\bar{\varepsilon}_{kl} - B'_{ijkl}\, d\bar{\varepsilon}_{kl} \tag{41}$$

where the matrices $D^{(A)}_{ijkl}, D^{(C)}_{ijkl}$ are the elastic stiffness matrix of the aggregate and the elasto-plastic stiffness matrix of the cement paste, respectively. The stress tensors $d\bar{\sigma}^{(A)}_{ij}, d\bar{\sigma}^{(C)}_{ij}$ are the increments in average stress on the micro level for aggregate and cement paste, respectively. Transferring the subscript of stain components i and j to k and l in Eq.(41), Eq.(41) can be written as

$$\begin{aligned}\delta_{ik}\delta_{jl}d\bar{\varepsilon}_{kl} &= C_1 \cdot D^{(A)}_{ijmn}{}^{-1} d\bar{\sigma}^{(A)}_{mn} + C_2 \cdot D^{(C)}_{ijmn}{}^{-1} d\bar{\sigma}^{(C)}_{mn} \\ &\quad - A'_{ijkl}\, d\bar{\varepsilon}_{kl} - B'_{ijkl}\, d\bar{\varepsilon}_{kl}\end{aligned} \tag{42}$$

Transferring the third and fourth terms on the right-hand side of Eq.(42) to the left-hand side, Eq.(42) can be written as

$$\begin{aligned}Q'_{ijkl}\, d\bar{\varepsilon}_{kl} &= C_1 D^{(A)}_{ijmn}{}^{-1} d\sigma^{(A)}_{mn} + C_2 D^{(C)}_{ijmn}{}^{-1} d\sigma^{(C)}_{mn} \\ Q'_{ijkl} &= R_{ijkl} + A_{ijkl} + B_{ijkl}\end{aligned} \tag{43}$$

where the matrix Q'_{ijkl} denotes the ratio of strain reduction due to cracks.

Now, the relation between the increment in average stress matrix on the macro level, $d\bar{\sigma}_{ij}$, and the increment in average stress matrix on the macro level, $d\bar{\sigma}^{(\alpha)}_{ij}$ $(\alpha = A, C)$, is defined as

$$\begin{aligned}d\bar{\sigma}^{(\alpha)}_{ij} &= C'^{(\alpha)}_{ijkl}\, d\bar{\sigma}_{kl} \\ \alpha &= A, C\end{aligned} \tag{44}$$

where $C'^{(\alpha)}_{ijkl}$ $(\alpha = A, C)$ is defined as the stress concentration matrix. The increment in average stress matrix on the macro level, $d\bar{\sigma}_{ij}$, can be written similarly to Eq.(26) and (27) using the incremental stress matrix on the micro level, $d\sigma_{ij}$, and the increment in average stress matrix on the micro level, $d\bar{\sigma}^{(\alpha)}_{ij}$ $(\alpha = A, C)$, as

$$d\bar{\sigma}_{ij} = \frac{1}{V}\int_V d\sigma_{ij}\, dV = C_1 \cdot d\bar{\sigma}^{(A)}_{ij} + C_2 \cdot d\bar{\sigma}^{(C)}_{ij} \tag{45}$$

In Eq.(45), it should be noted that continuous changes in stress at each interface as shown in Fig.2 occur and that the ratio of crack band volume to controlled volume is already equal to zero ($C_3 = 0$). Substituting Eq.(44) into Eq.(45), the relation between the stress concentration matrices for aggregate and cement paste can be written as

$$C_1 C'^{(A)}_{ijkl} + C_2 C'^{(C)}_{ijkl} = I_{ijkl} \tag{46}$$

where the matrix I_{ijkl} is the unit matrix.

Moreover, substituting Eq.(44) into Eq.(43), Eq.(43) can be rewritten as

$$d\bar{\sigma}_{ij} = (C_1 \cdot D^{(A)-1}_{ijst} C'^{(A)}_{stop} + C_2 \cdot D^{(C)-1}_{ijst} C'^{(C)}_{stop})^{-1} Q'_{opkl}\, d\bar{\varepsilon}_{kl} \tag{47}$$

Finally, the elasto-plastic matrix of the concrete body on the macro level, D_{ijkl}, which is related by the increment in average stress on the macro level, $d\bar{\sigma}_{ij}$, and strain on the macro level, $d\bar{\varepsilon}_{ij}$, can be written as

$$D_{ijkl} = (C_1 \cdot D_{ijst}^{(A)^{-1}} C'^{(A)}_{stop} + C_2 \cdot D_{ijst}^{(C)^{-1}} C'^{(C)}_{stop})^{-1} Q'_{opkl} \tag{48}$$

Here, solving the simultaneous equation of Eq.(48) and Eq.(46), the stress concentration matrices $C_{ijkl}^{(A)}, C_{ijkl}^{(C)}$ as shown in Eq.(48) can be written as

$$C'^{(C)}_{ijkl} = \left\{ C_2 \cdot \left(D_{ijqr}^{(C)^{-1}} - D_{ijqr}^{(A)^{-1}} \right) \right\}^{-1} \left(Q'_{qrop} - D_{qrst}^{(A)^{-1}} D_{stop} \right) D_{opkl}^{-1}$$
$$C'^{(A)}_{ijkl} = \left(I_{ijkl} - C_2 \cdot C'^{(C)}_{ijkl} \right) / C_1 \tag{49}$$

Analysis proceeds as follows. The stress concentration matrices given as Eq.(49) are updated due to the substitution the elasto-plastic stiffness matrix just at before step and substituting the updated stress concentration matrix into the elasto-plastic stiffness matrix of Eq.(48), The elasto plastic-stiffness matrix is then updated and, finally, the force imbalance is calculated from the internal forces and external forces on the structural body. Further, the calculation is iterated until the unbalanced forces fall within a specific error by the modified Newton Raphson method.

This sets up, the formulation of a permeability matrix and elasto-plastic stiffness matrix for a non-homogeneous material such as cracked concrete. A practical calculation will be carried out using analytical theory for water migration in concrete as a homogeneous material developed by authors[8] incorporated the above formulations.

This model of water migration can estimate the transition process by which concrete varies from a homogeneous to non homogeneous body as well as a mixed state arising from the loading history. That is, the model can estimate the permeability matrix and elasto-plastic stiffness matrix as they vary with the degree of damage, or crack width. Moreover, the characteristics of water migration in the material can be obtained when only the initial conditions of the material, such as initial permeability, young's modulus, internal friction angle, and cohesion in the plastic region of the cement paste, are given.

Such an analytical method for water migration has never been proposed in the past. However, to make use of the proposed model, the material parameters a, b, c, d as shown in Eq.(10) and Eq.(35) must be determined, and hence determination of these parameters will be done in Sections 4 and 5.

3. NUMERICAL SIMULATION USING DEVELOPED MODEL

3.1 Analytical Model and Conditions

The analytical model is a one-eighth prism specimen with a side length of 8.86cm and a height of 20.0cm, as shown in Fig.6. Surface cracks are introduced into this prismatic specimen to show the influence of the developed model on the characteristics of water migration in cracks and hence these cracks are taken into account in the analytical model. A uni-axial compressive load is applied to the top surface of the model, and differences in the coefficient of

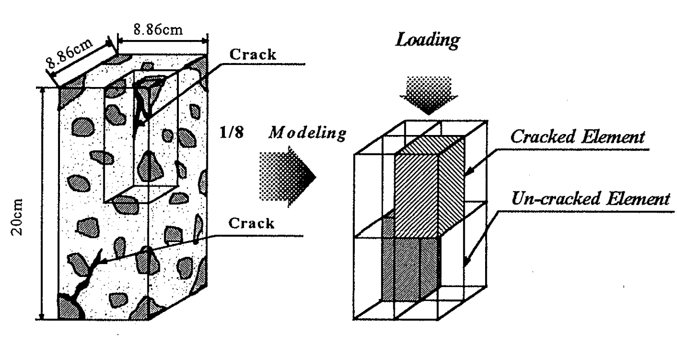

Fig. 6 Numerical Simulation Model

Table 1 Material Parameters Using in Simulation

Compressive Strength (MPa)	Young's Modulus (MPa)	Initial Permeability ($cm/\sec$)	Friction Angle (°)	Initial Cohesion (MPa)
14.0	5.2×10^3	1.67×10^{-8}	29.0	3.5

permeability, total stress, and pore water pressure in cracked and uncracked elements are elucidated. The boundary conditions are assumed to be a uni-axial displacement state with pore water-drained.

The mechanical characteristics of concrete used in the analysis, including uni-axial compressive strength, young's modulus, initial coefficient of permeability, internal friction angle, and initial cohesion of cement paste[6], are shown in Table 1. Here, Young's modulus[8] is the effective Young's modulus. Further, material parameters a,b in Eq.(10) and c,d in Eq.(35) are assumed to take values of 10^3 and 10^{-6}, respectively.

3.2 Changes in Coefficient of Permeability and Characteristics of Water Migration

The stress state and pore water pressure in cracked and uncracked elements will be discussed on the basis of changes in the coefficient of permeability when a compressive load is applied to the top surface of the specimen shown in Fig. 6. Analytical results are shown in Fig. 7. Figures. 7(a), (b) and (c), respectively, show the relationships between coefficient of permeability and total strain, total stress and total strain, and pore water pressure and total strain. The analytical results for uncracked and cracked elements are shown by solid and dotted lines, respectively.

As shown in Fig. 7(a) and (b), a parabolic increase in the coefficient of permeability of a cracked element occurs when the total strain reaches about 1800 μ in which concrete varies from elastic to plastic. That the maximum value is 4.0×10^{-6} cm/sec, which corresponds to about two hundred times the initial permeability in the range of the current analysis. It seems that the change in permeability influences the characteristics of pore water pressure. Namely, a sudden increase in pore water pressure occurs due to the relatively small initial permeability and it reaches a maximum value when the total strain reaches about 1800 μ Then a sudden decrease occurs due to the increase in permeability and the plastic volumetric expansion caused by increasing crack width, until and finally the pore water pressure takes a negative (tension) value.

Above all, it is noted that changes in the permeability and water migration characteristics of concrete can be estimated automatically if only the mechanical characteristics are input into the model. However, the material parameters a,b,c,d in Eq.(10) and Eq.(35) must be determined in order to use the developed model in detail. In sections 4 and 5, there material parameters will be determined due to the comparison of the experimental and analytical results. Moreover, the relation between coefficient of permeability and crack pattern will be estimated analytically.

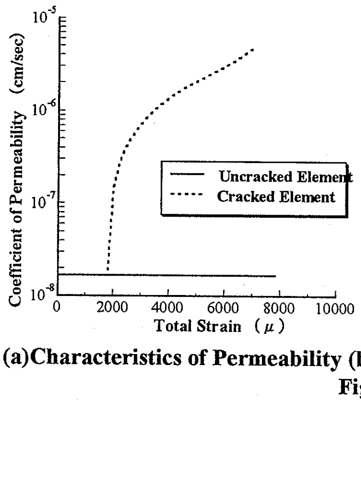

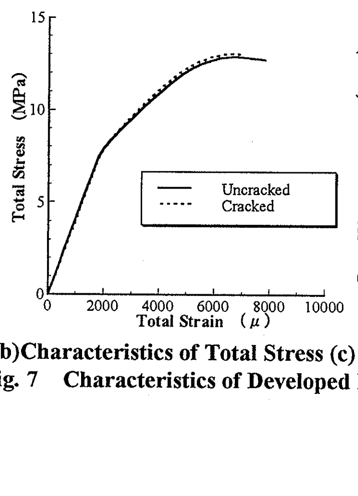

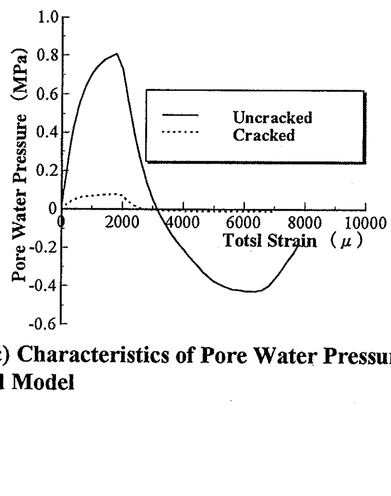

(a)Characteristics of Permeability (b)Characteristics of Total Stress (c) Characteristics of Pore Water Pressure

Fig. 7 Characteristics of Developed Model

4. PAST EXPERIMENTAL FORMULAS FOR LEAKAGE IN

4.1 Leakage Experiment by Watabe

Watabe performed an experiment to measure the leakage of water from cracks and joints due to external forces for each specimen's type in the case of the radioactive waste disposal facility shown in Fig.8 in order to quantitatively estimate durability. Specimen A is a model assuming that cracks occur due to earthquake forces, and cracks were introduced by a reversed bending load. Specimen F is a model assuming that the cracks occur due to ground subsidence, and the cracks were introduced by a bending load. Specimens B, C, D, and E are models assuming that the vertical and horizontal joints, respectively. The analysis of water migration was performed for the specimen of type A in the next chapter. this specimen is a plate of width 40 cm, length 60 cm, and height 15 cm. PC bars were placed perpendicularly to the single passing crack shown in Fig.9 and the width of the single passing crack is uniform at each cross section.

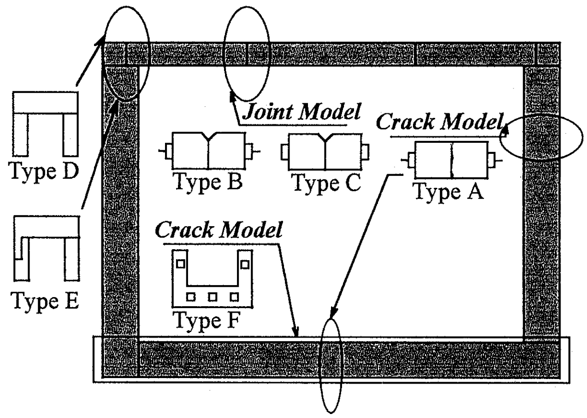

Fig. 8 Modeling of Radioactive Waste Disposal Facility[4]

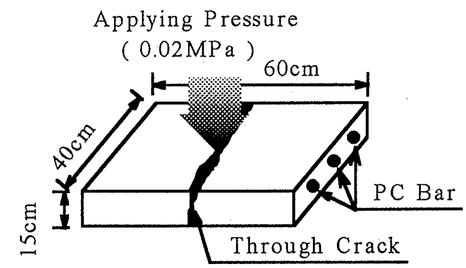

Fig. 9 Experimental Specimen of Type A[4]

Water's experimental results of leakage for specimen A are shown in Fig.10 for the case of a water pressure of 20 kPa applied to the top surface of the specimen shown in Fig.9. Figure.10 shows the relationship between leakage per unit length of the single passing crack and crack width. In this figure, the experimental results are shown by circles while the results using equations proposed Watabe, Ishikawa, and Ito (which are shown below) were shown by solid, dotted, and broken lines, respectively.

$Q = K \times \omega^3$: Proposed by Ishikawa (50)

$Q = K \times (\omega - \omega_0)^{3.2}$:Proposed by Watabe (51)

$Q = K \times (\omega - \omega_0)^3$:Proposed by Ito et al. (52)

Where, parameters K, Q, ω, ω_0 are as follows.

$$K = \frac{P}{12 \eta D \sigma}$$

Q : leakage $(cm^3 / \mathrm{sec} \cdot cm)$

ω : crack width (cm)

ω_0 : critical crack width at which leakage does not occur

P : applied pressure ($\times 10^{-1}$ MPa)

η : coefficient of water viscosity ($\times 10^{-1}$ $MPa \cdot \mathrm{sec}$)

D : water course length (cm)

σ : crack parameter

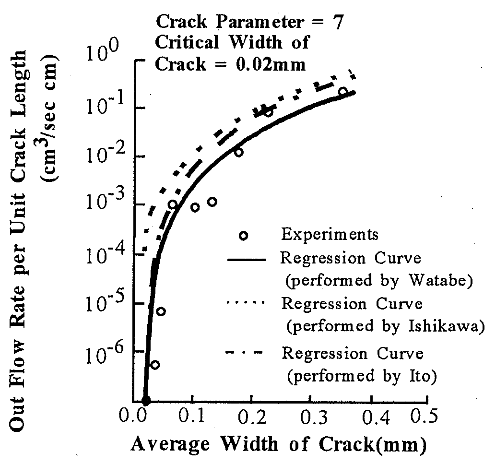

Fig. 10 Experimental Results of Leakage Water

The equation proposed by Watabe is regression curves of experimental results in which the only critical crack width at which leakage dose not occur, is introduced into Ishikawa's equation. Ishikawa's equation is defined by incorporating the crack parameter into the solution obtained theoretically from the Navier-Stokes equation of motion by assuming a laminar flow between parallel plates. The value of the crack parameter is reported by Watabe to be 7.0. As shown in Fig.10, Watabe's equation shows good agreement with the experimental results due to the regression curve of experimental results. On the other hand, Ishikawa's equation shows higher values on the whole compared with the experimental results, and there is a particularly large discrepancy in the range below a crack width of 0.05 mm since the critical crack width isn't present. Ito's equation gives values between Ishikawa's and Watabe's, and is a little on the high side compared with the experimental results. Particularly, its value falls to Ishikawa's equation as the crack width becomes larger due to the only introduction of critical crack width to Ishikawa's equation.

4.2 Leakage Experiment by Ito et al

Ito performed a leakage experiment with water under higher pressure (200.0 kPa) compared with the experiments by Watabe and Ishikawa (20 kPa) to predict the water-tightness of concrete structures facing the serious problem of seepage in deeper underground space and in the development of waterfront areas. The specimen is a plate of width 34 cm, length 50 cm and height 15 cm, as shown in Fig.11. Cracks were introduced at the age of 14 days by applying a reversed bending load and the crack width was controlled by PC bars placed on the outer faces of the specimen. Compressive water pressure was applied on the top surface of the specimen with values of 2.0 kPa and 200.0 kPa. The experimental results are shown in Fig.12. Figures.12(a), (b) show the relationship between water leakage per unit length of crack and crack width with water pressures of 2.0 kPa and 200.0 kPa, respectively. In this figure, the experimental results are shown by circles and the equations proposed by Ito, Ishikawa, and Watabe are shown by solid, dotted, and broken lines, respectively. As shown in Fig.12, Ito's equation, which is a regression curve of experimental results, shows a good agreement with the experimental results as compared with the other equations. On the other hand, Ishikawa's equation shows the higher value on the whole compared with the experimental results similarly to the tendency shown in Watabe's experimental results with particularly great differences occurring in the region of crack width below 0.01 mm in Fig.12(a) and below 0.05 mm in Fig.12(b). Watabe's equation gives lower values compared with the experimental results as the crack width becomes larger.

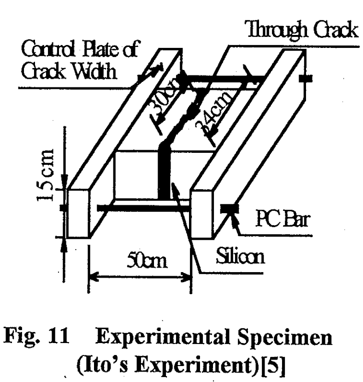

Fig. 11 Experimental Specimen (Ito's Experiment)[5]

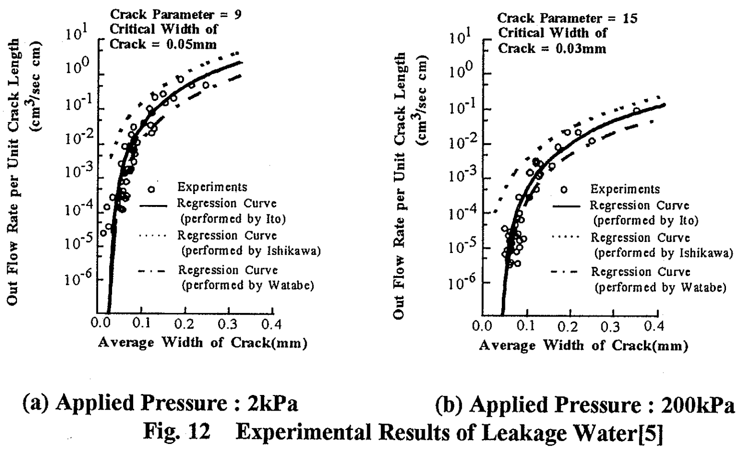

(a) Applied Pressure : 2kPa (b) Applied Pressure : 200kPa

Fig. 12 Experimental Results of Leakage Water[5]

4.2 Comparison of Each Equation

As mentioned above, Ishikawa's equation gives higher values on the whole compared with the experimental results, and particularly great differences occur as the crack width becomes smaller. Watabe's equation gives lower values as the crack width increases but agrees well with the experimental results in the region of crack width below 0.1 mm due to the introduction of the critical crack width. Ito's equation gives intermediate values between Ishikawa's and Watabe's equation, providing the best fit among these proposed equations.

Each of these proposed equations is expressed in almost the same form and all use a crack parameter. This crack parameter is defined as material constant expressing changes in water course length, frictional resistance, and tortuosity with crack roughness. According to Ito's experiments shown in Fig.12, the crack parameter takes a value rising from 9 to 15 as the applied water pressure becomes higher. However, though the value of water pressure in Watabe's experiments was within the range used in Ito's experiments, the crack parameter obtained by Watabe was 7.0, which is smaller that that obtained by Ito. Therefore, it should be noted that, according to the choice of crack parameter, predictions of water leakage vary greatly, i.e., in predicting leakage from concrete in which the crack parameter was not measured, the crack parameter is uncertain and hence the reliability of the equations is lost. The fact that the crack parameter is an uncertain factor is confirmed from Ishikawa's experiment shown in Fig.13. This shows the distribution of crack parameters obtained using the same concrete. As shown in Fig.6, the value of crack parameter is distributed in the wide range of 3 to 15, and its value can not be decided uniquely. Hence, it should be noted that there is a serious problem in deciding the crack parameter, thus leading to problems with equations which make use of the crack parameter. In the next section, the relationship between permeability and crack width, in which there is no uncertainty, will be estimated analytically and experimentally by an analytical investigation of Watabe's experiments. Moreover, applying the resulting relations to Ito's experiments, the applicability of the relationship between the permeability and crack width will be evaluated.

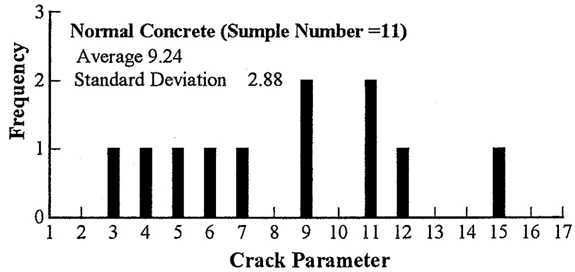

Fig. 13 Distribution of Crack Parameter (Ishikawa Experiments)[3]

5. ANALYTICAL ESTIMATION OF PERMEABILITY AND ITS APPLICABILITY

The permeability of concrete as a homogeneous material mainly depends on material properties such as water-cement ratio, maximum aggregate size, and age, and these properties are the main factors which determine the maximum continuous pore size. Namely, it seems that the permeability of concrete as a homogeneous material is approximately determined by the width of the water course. On the other hand, the permeability of concrete as a non-homogeneous material is determined by the crack width and crack surface roughness in addition to the these properties. Therefore, the experimental water leakage results obtained by Watabe, Ito, and Ishikawa can be used to predict permeability with the changes in crack width. In this section, the developed analytical model is first applied to the experimental results obtained by Watabe and shown in Fig.10. In this way, permeability with changes in crack width will be estimated analytically. Secondly, an analytical investigation of the results obtained by Ito and shown in Fig.12 will be performed using the obtained relation of permeability and crack width, allowing the applicability of the developed model and its relation to be evaluated.

5.1 Analytical Estimation of Permeability

The specimen used in the experiments performed by Watabe applied the developed analytical model is shown in Fig.9 and it is called as type A in pit model shown in Fig.8. A single passing crack was introduced by applying reserved bending load and the crack width is the average value measured by the contact-type strain gages on each cross section. The method of applying the developed model to the experimental results for the type A specimen is such that the analytical model represents one quarter of the specimen, as shown in Fig.14, and the forced displacement under uni-axial tension was induced by the displacement control becoming the total discontinuity of displacement shown in Eq.(34) up to the appointed value. Leakage from the bottom surface of the specimen was then analyzed at a water pressure of 20 kPa on the top surface of analytical model, as shown in Fig.14. This leakage is decided uniquely by the initial permeability of concrete as a homogeneous material and the degree of reducing rate of hydraulic gradient a,b shown in Eq.(10). Hence, since the permeability estimated by analysis varies with changes in crack width and with the material parameters a,b, the analysis with the variables of material parameters a,b is repeated such that the differences of leakage water in the experimental and analytical results become within the appointed error. When the differences of leakage water becomes within the appointed error, the permeability corresponding to the crack width is decided analytically and at the same time the material parameters a,b are decided. The material parameters a,b are constants at each analytical step and are values of crack width's own. Though the material parameters denoting the degree of reducing rate of hydraulic gradient a,b and the degree of localized strain c,d are, strictly, different at the interfaces the aggregate and cement paste and between the cement paste and crack band, the difference between the interfaces may be ignored after cracking and hence these parameters are assumed to be equal, i.e., $a=b$ and $c=d$. The material parameters c,d are given a value of 10^{-6} due to the analytical estimation of the result obtained by uni-axial compressive tests.

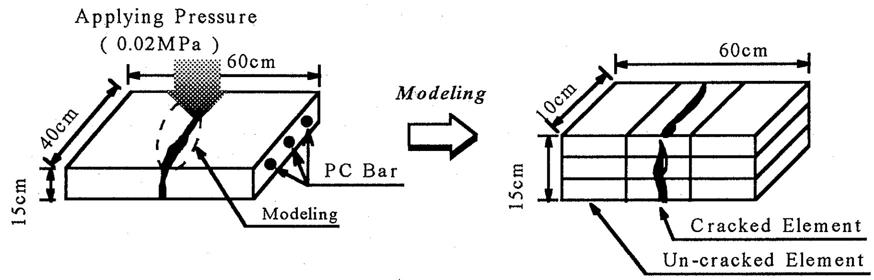

Fig. 14 Analytical Model of Watabe's Experiment

A practical calculation of changes in coefficient of permeability and water leakage in concrete as a non-homogeneous material can be done due to the incorporating the developed model as a non homogeneous material to the governing equation for water migration in homogeneous material which is coupled of the force equilibrium equation and mass conservation law developed by authors[8]. The analytical model for water migration in a homogeneous material is summarized as follows. CSH gel particles and the aggregate particles are considered to be elastic. However, when mixed they may be subject to shear deformation as the relative locations of particles changes, so it may be reasonable to assume that it is a hardening visco-plastic material with the pore volume fully saturated or partially saturated with water as age increases. Ultimately, the governing equation for water migration is expressed as the coupled equation of the force equilibrium and mass conservation laws for pore water, and hence the characteristics of water migration in concrete can be obtained theoretically by solving simultaneous equations in which the nodal displacement vector and nodal pore water pressure are unknown. In the modeling of concrete, a Drucker-Prager failure function is incorporated and it is assumed that the failure surface varies with the degree of damage[6] shown in Eq.(10) in the stress space. The applicability of the developed model for water migration in concrete as a homogeneous material was confirmed through comparison with the experimental results for pore water pressure in concrete obtained by the authors[9].

a) Material Parameters the Analysis

Material parameters such as compressive strength, tensile strength, Young s modulus, initial concrete permeability, internal friction angle, cohesion of cement paste, and bulk modulus of water, yield stress, Young s modulus of PC bars have to be determined to perform the above analysis. These parameters of concrete are shown in Table.2, the bulk modulus of water is $2200(MPa)$ and the yield stress, Young s modulus of PC bars are $950(MPa)$, $2.0\times10^5(MPa)$, respectively.

Table 2 Material Parameters of Concrete Using in Analysis

Compressive Strength (MPa)	Tensile Strength (MPa)	Young's Modulus (MPa)	Initial Permeability $(cm/\sec)$	Friction Angle $(°)$	Initial Cohesion (MPa)
57.6	6.2	3.6×10^4	1.67×10^{-11}	29.0	3.9

For the compressive and tensile strength of concrete, the experimental results obtained by Watabe are used and the Young s modulus of concrete was predicted according to the following equation:

$$E_c = 47434 \times \sqrt{f'_c} \quad (MPa) \tag{53}$$

f'_c : uni-axial compressive strength of concrete (MPa)

For the internal friction angle and cohesion of cement paste, the experimental results obtained in tri-axial compressive tests[10] on cylindrical specimens with a diameter of 5 cm and a height of 10 cm were used. The tests were performed under drained conditions as regards pore water. Hence, it seems that the pore water pressure occurring in concrete is almost zero judging by the relatively small specimen s size and drained condition for pore water. That is, the effect of pore water pressure on internal friction angle and cohesion can be ignored. In the analysis, the internal friction angle and cohesion were 29 degrees and one quarter of the compressive strength obtained by the uni-axial compressive strength tests, respectively.

The initial permeability at the age of 28 days, i.e., the permeability of concrete as a homogeneous material, was predicted from the permeability experiments performed by J.Murata and T.C.Powers, as shown in Figs.15 and 16.

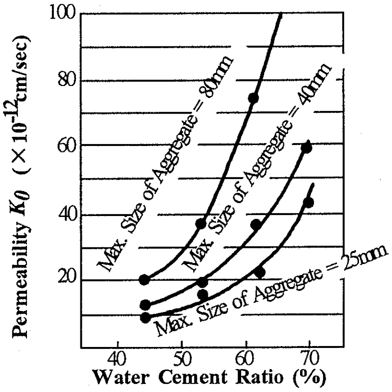

Fig. 15 Permeability Tests (performed by Murata)[1]

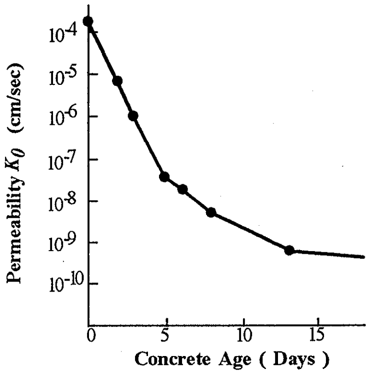

Fig. 16 Permeability Tests (performed by T.C.Powers)[2]

b) Analytical results of Permeability

The analytical and experimental results of leakage with the application of a water pressure 20.0 kPa to the top surface of the specimen are shown in Fig.17 which is the relationship between the flow rate Q' and crack width ω. Analytical and experimental results are shown by white circles and black circles, respectively. The analytical results show good agreement with the experimental results due to the accurate estimation of the material parameters a,b shown in Eq.(10). At the same time, the permeability matrix corresponding to each crack width was chosen due to the good agreement of the analytical results with the experimental results for leakage. The analytical estimation of permeability parallel to the crack surface is shown in Fig.18 which shows the relationship between permeability and crack width with the permeability (vertical axis) on a logarithmic scale.

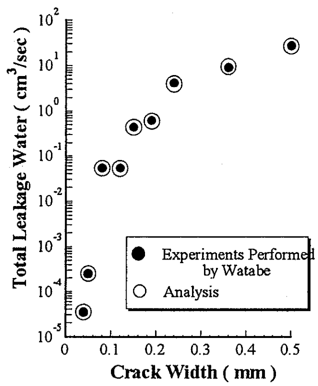

Fig. 17 Total Leakage Water

As shown in Fig.18, a parabolic increase in permeability occurs with increasing crack width, with permeability taking a value of 10^{-5} and $10^{-3} cm/\sec$ at crack widths of 0.1mm and 0.3mm, respectively. The permeability of $10^{-3} cm/\sec$ at a crack width of 0.3mm corresponds to materials such as sand in soil mechanics. The normalized permeability K/K_0 is shown in Fig.19 indicating values of 10^6 and 10^8 times the initial permeability at crack widths of 0.1mm and 0.3mm, respectively. Further, the results denoted the axis of crack width (horizontal axis) with logarithm are shown in Fig.20. Here, it should be noted that the relation between permeability and crack width can be regressed with three straight lines as follows.

$$\begin{aligned}
&\log(K/K_0) = 0 && 0.0 \le \omega < 0.015(mm) \\
&\log(K/K_0) = 6.349 \cdot \log\omega + 11.580 && 0.015 \le \omega < 0.24(mm) \\
&\log(K/K_0) = 2.570 \cdot \log\omega + 9.238 && 0.24(mm) \le \omega
\end{aligned} \tag{54}$$

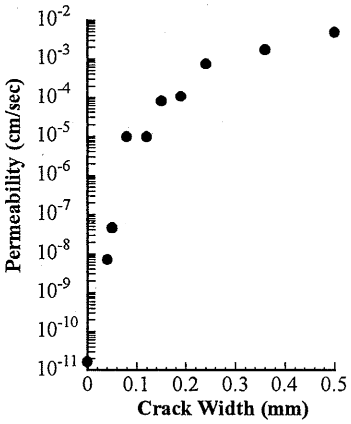

Fig. 18 Permeability with Crack with Crack Width

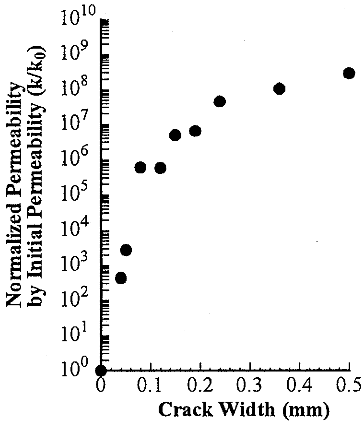

Fig. 19 Normalized Permeability (Horizontal Axis : Linear)

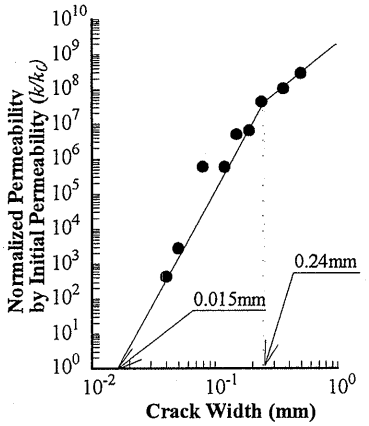

Fig. 20 Normalized Permeability (Both axes : Logarithm)

Assuming little water leakage for concrete as a homogeneous material, it should be noted that the intersection point of the above lines and the horizontal axis indicates the critical crack width at which leakage does not occur. This is a value of 0.015mm in the analytical results, almost the same as that in Watabe s experiment (0.02mm). However, this critical crack width will be defined as the hardened concrete and hence the assumption that leakage will not occur in homogeneous concrete is not valid in the case of high initial permeability and high water content, such as young age concrete, and we should pay attention to the possibility of leakage in concrete without cracks[11]. At a crack width of 0.24mm, or the intersection of the last two regression lines, it seems that the crack width corresponds to the critical Reynolds number at which flow mares from laminar to turbulent according the experimental results obtained by Yanag et al.[12] in which the crack width taking a value of 0.2mm is corresponding to that number.

c) Determination of Material Parameters

The material parameters a,b in Eq.(10) were determined when good agreement was obtained between analytical results for water leakage and experimental results, as shown in Fig.17. The relationship between such material parameters and crack width are shown in Fig.21, where the horizontal and vertical axes are logarithmic. As shown in Fig.21, the relation was regressed with three straight lines as follows.

$$
\begin{aligned}
&\log a = 0 && 0.0 \le \omega < 0.015(mm) \\
&\log a = 6.005 \cdot \log \omega + 10.953 && 0.015 \le \omega < 0.24(mm) \\
&\log a = 1.141 \cdot \log \omega + 7.938 && 0.24(mm) \le \omega \\
&a = b &&
\end{aligned}
\qquad (55)
$$

If the applicability of permeability obtained by analysis can be estimated, it should be noted that the reliability of the material parameters a,b in Eq.(10) will be also confirmed. Namely, the applicability of the proposed permeability will be confirmed, and changes in the permeability of concrete as it changes from a homogeneous to non-homogeneous material, changes in permeability with changes in crack width, and the characteristics of water migration in non-homogeneous material can be predicted automatically by substituting the above equation into Eq.(10).

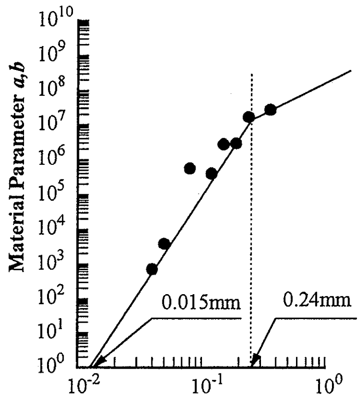

Fig. 21 Material Parameters

5.2 Estimation of Applicability of Proposed Permeability

The relationship between permeability and crack width could be estimated analytically the analytical estimation of experimental results of water leakage with a water pressure of 20.0 kPa a the top surface of specimen A in Watabe s experiments. In this section, by performing an analytical estimation of water leakage for the experiments performed by Ito, the applicability of the proposed permeability will be verified. The experimental specimen used in Ito s experiment was a plate as shown in Fig.11, and cracks were introduced by applying a reversed reserved bending load. The crack width is the average value measured by contact strain gages placed on several cross sections, and the average crack width was controlled by PC bars placed on both faces of specimen as shown in Fig.11. The proposed permeability is applied to Ito s specimen modeling one third of the experimental specimen as shown in Fig.22, and leakage was calculated when water pressures of 2.0 and 200.0 kPa are applied to the top surface of the model. The initial value of permeability is $1.67 \times 10^{-11} cm/\sec$ in an uncracked element and as a value calculated in Eq.(54) corresponding to the crack width in cracked element. If the elasticity of the concrete specimen, is assumed the material parameters needed in the analysis are only Young s modulus of the concrete, initial permeability of the uncracked and cracked concrete, and the bulk modulus of water. The values of these parameters are shown in Table.2.

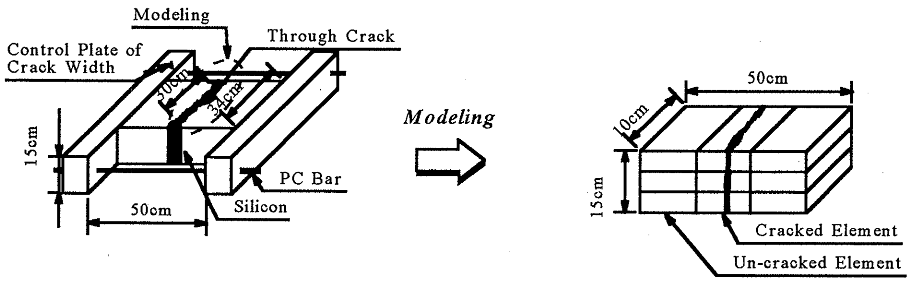

Fig. 22 Analytical Model of Ito's Experiment

The analytical results are shown in Fig.23. This is the relationship between leakage per unit crack length and average crack width. Figures.23(a) and (b) show the results of applying water pressure at 2.0 and 200.0 kPa, respectively. In this figure, the analytical results are shown by black circles, the experimental results by white circles and the regression curve obtained by Ito by a solid line, respectively.

The analytical results show good agreement with the experimental results and hence the permeability, i.e., Eq.(54), is estimated accurately. Moreover, the developed model for water migration does not contain such uncertainties as the crack parameter, and the effect of watercourse length, frictional resistance, and tortuosity, i.e., the roughness of the crack surface, are already introduced into the relationship between permeability or material parameters a,b and crack width due to the good agreement obtained in Fig.17. Hence, using the relation shown in Eq.(54) without any consideration of uncertainties such as crack parameter, an accurate estimation of water leakage from a cracked or

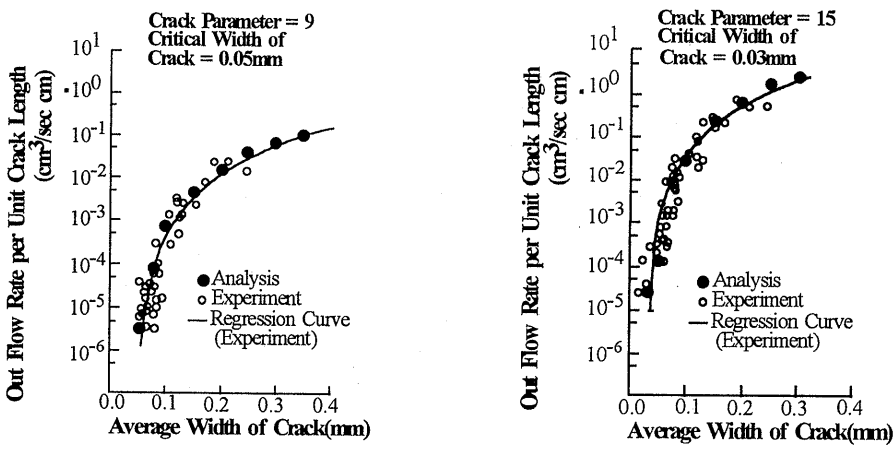

(a) Applied Pressure : 2.0kPa **(b) Applied Pressure : 200.0kPa**

Fig. 23 Analytical Estimation for Leakage Water Experiments (Compared with Ito's Experiments)

uncracked concrete specimen can be. However, we can not generalize the applicability of the developed model to experiments other than Ito s. The wider applicability of the developed model must now be confirmed by comparison with many other experiments.

6. PROPOSAL FOR UNIFIED WATER MIGRATION MODEL

A unified water migration model for concrete having uncracked and cracked regions is proposed as follows. The unified water migration model can automatically estimated water leakage and the characteristics of water migration in concrete as a homogeneous, non-homogeneous, or mixed material if only the initial conditions of the materials, such as initial permeability, Young s modulus of the concrete, internal friction angle, and cohesion of cement paste are given. Moreover, the unified water migration model can be applied to concrete with a complicated crack pattern, such as the smeared cracks that occur in real concrete structures due to external loading.

Conclusions

In this study, a unified water migration model for concrete as both a homogeneous and non-homogeneous material is developed. Using the unified water migration model, the relationship between permeability and crack pattern was estimated analytically and the applicability of the unified water migration model and the above relation were confirmed. The following conclusions were reached:.

(1) The unified water migration model for concrete as a homogeneous, non-homogeneous, or mixed material is proposed.

(2) A relationship between permeability and crack width was proposed.

Notations

Q_{in}	:	inflow rate
Q_{out}	:	outflow rate
ΔV	:	accumulation rate
v_i	:	flow velocity of pore water
σ_{ij}	:	total stress in macro level
σ_{ij}'	:	effective stress
p	:	pore water pressure
m_{ij}	:	$[1 \ 1 \ 1 \ 0 \ 0 \ 0]^T$
V	:	controlled volume
$d\bar{\iota}_i$	:	increment of average hydraulic gradient vector in macro level
$d\iota_i$	:	incremental hydraulic gradient vector in micro level
C_1	:	rate of volume of aggregate to the controlled volume
C_2	:	rate of volume of cement paste to the controlled volume
C_3	:	rate of volume of crack band to the controlled volume
$d\bar{\iota}_i^{(A)}$	:	increment of average hydraulic gradient vector in micro level of aggregate
$d\bar{\iota}_i^{(C)}$	:	increment of average hydraulic gradient vector in micro level of cement paste
$d\bar{\iota}_i^{(CB)}$	:	increment of average hydraulic gradient vector in micro level of crack band
X_i	:	degree of discontinuity of hydraulic gradient at each interface in micro level
$dh^{(\alpha)}$	:	increment of total water head in micro level $\alpha = A,C,CB$
$dz^{(\alpha)}$	:	increment of potential head in micro level $\alpha = A,C,CB$
$dP^{(\alpha)}$	:	increment of pore water pressure in micro level $\alpha = A,C,CB$
γ_w	:	weight per unit volume of water

n_i	:	unit normal vector at crack band surface
t_i	:	unit tangential vector at crack band surface
$[dh]_A^C$	:	discontinuity of total water head between the aggregate and cement paste in micro level
$[dh]_C^{CB}$	:	discontinuity of total water head between the cement paste and crack band in micro level
$d\iota_n$	:	components of hydraulic gradient on the normal direction at crack surface
$d\iota_t$	:	components of hydraulic gradient on the horizontal direction at crack surface
a	:	degree of discontinuity of hydraulic gradient between aggregate and cement paste. i.e., the material parameter which express the degree of reducing ratio of hydraulic gradient with crack width
b	:	degree of discontinuity of hydraulic gradient between cement paste and crack band. i.e., the material parameter which express the degree of reducing ratio of hydraulic gradient with crack width
ω	:	damage parameter
$\Omega_{(\theta)}^{A-C}$	:	contact density function of cracks at the interface of aggregate and cement paste
$\Omega_{(\theta)}^{C-CB}$	:	contact density function of cracks at the interface of cement paste and crack band
A_t^{A-C}	:	whole surface area per unit crack plane at the interface between aggregate and cement paste
A_t^{C-CB}	:	whole surface area per unit crack plane at the interface between cement paste and crack band
$d\overline{v}_i^{(A)}$	:	increment of average flow velocity in aggregate in micro level
$d\overline{v}_i^{(C)}$	:	increment of average flow velocity in cement paste in micro level
$d\overline{v}_i$	:	increment of average flow velocity vector in macro level
dv_i	:	increment of flow velocity vector in micro level
$K_{ij}^{(A)}$	:	permeability matrix of aggregate in micro level
$K_{ij}^{(C)}$	:	permeability matrix of cement paste in micro level
K_{ij}	:	permeability matrix of concrete body in macro level
$C_{ij}^{(A)}$	:	concentration matrix of flow velocity in aggregate
$C_{ij}^{(C)}$	:	concentration matrix of flow velocity in cement paste
I_{ij}	:	unit matrix
$d\overline{\varepsilon}_{ij}$	:	increment of average strain in macro level
$d\varepsilon_{ij}$	:	incremental strain in micro level
$d\overline{\varepsilon}_{ij}^{(A)}$	:	increment of average strain in micro level of aggregate
$d\overline{\varepsilon}_{ij}^{(C)}$	:	increment of average strain in micro level of cement paste
$d\overline{\varepsilon}_{ij}^{(CB)}$	:	increment of average strain in micro level of crack band
X_{ij}	:	degree of discontinuity of strain at each interface in micro level
$d\overline{u}_i^{(\alpha)}$	:	incremental displacement vector in micro level $(\alpha = A, C, CB)$
$[du_i]_A^C$	:	discontinuity of the incremental displacement vector between aggregate and cement paste in micro level
$[du_i]_C^{CB}$	:	discontinuity of the incremental displacement vector between cement paste and crack band in micro level
du_n	:	component of displacement on the normal direction at crack surface
du_t	:	component of displacement on horizontal direction at crack surface

$\left[du_n\right]_A^C$: degree of discontinuity of incremental displacement on the normal direction at crack surface between aggregate and cement paste

$\left[du_t\right]_A^C$: degree of discontinuity of incremental displacement on the horizontal direction at crack surface between aggregate and cement paste

$\left[du_n\right]_C^{CB}$: degree of discontinuity of incremental displacement on the normal direction at crack surface between cement paste and crack band

$\left[du_t\right]_C^{CB}$: degree of discontinuity of incremental displacement on the horizontal direction at crack surface between cement paste and crack band

$d\varepsilon_n$: component of incremental strain in micro level on the normal direction at crack surface

$d\varepsilon_t$: component of incremental strain in micro level on the horizontal direction at crack surface

c : degree of discontinuity of displacement between aggregate and cement paste i.e., the material parameter which express the degree of strain localization due to cracks

d : degree of discontinuity of displacement between cement paste and crack band i.e., the material parameter which express the degree of strain localization due to cracks

ω_1, ω_2 : damage parameter ($=\omega$)

$d\bar{\sigma}_{ij}^{(A)}$: increment of average stress in aggregate in micro level

$d\bar{\sigma}_{ij}^{(C)}$: increment of average stress in cement paste in micro level

$d\bar{\sigma}_{ij}$: increment of average stress matrix in macro level

$d\sigma_{ij}$: increment of stress matrix in micro level

$D_{ijkl}^{(A)}$: elastic stiffness matrix of aggregate in micro level

$D_{ijkl}^{(C)}$: elasto plastic stiffness matrix of cement paste in micro level

$C'^{(A)}_{ijkl}$: stress concentration matrix in aggregate

$C'^{(C)}_{ijkl}$: stress concentration matrix in cement paste

D_{ijkl} : elasto plastic matrix of concrete body in macro level

I_{ijkl} : unit matrix

References

[1] Murata, J. : Studies on the Permeability of Concrete, *Trans. of JSCE*, No.77, Nov., pp.69-103, 1961

[2] Powers, T. C., Copeland, L. E., Hayes, J. C., and Mann, H. M. : Permeability of Portland Cement Paste, *ACI Journal*, No.51-14, Nov., pp.285-298, 1954

[3] Ishikawa, K. : Water Leakage at Cracks in a Mortar and Concrete Wall Structure, *Proc. of Architectural Institute of Japan*, pp.277-278, 1977 (in Japanese)

[4] Watabe, N. : Study on Water tightness of Concrete Pit for Radioactive Waste Disposal Facility, *Report of Central Research Institute*, U87023, 1987 (in Japanese)

[5] Ito, T et al. : Water Leakage from Concrete with a passing crack under High Water Pressure, *Proc. of JSCE Annual Conference*, Vol.5, pp.412-413, 1989 (in Japanese)

[6] Wu, Z. S., and Tanabe, T. : A Hardening-softening Model of Concrete Subjected to Compressive Loading, *Journal of Structural Engineering, Architectual Institute of Japan*, Vol.36B, pp.153-162, 1990

[7] Farahat, A. M. : Development of Concrete Models Based on the Micromechanics of Granular Materials, *Doctoral thesis at Nagoya University*, 1992

[8] Oshita, H. and Tanabe, T. : Analytical Study on Predicting Pore Water Pressure Occurring in Concrete and Its Effects, *Pro. of JSCE,* No.526 / V-29, Nov., pp.29-41, 1995 (in Japanese)

[9] Oshita, H. and Tanabe, T. : Experimental Study on Measuring Pore Water Pressure Occurring in Concrete and Its Effects, *Pro. of JSCE,* No.514 / V-27, May, pp.75-84, 1995 (in Japanese)

[10] Inoue, T. : Study on the Deformational Behavior of Concrete at Early Ages, *Master's Thesis at Nagoya University*, 1990 (in Japanese)
[11] Ishikawa, Y. : Deformational Analysis of Concrete as Saturated Porous Permeable Material at Early Ages, *Master's thesis at Nagoya University*, 1993
[12] Yanagi, H. : Prediction of Water Leakage from Crack in Concrete, *Proc. of JSCE Annual Conference*, Vol.5, pp.650-651, 1994 (in Japanese)